Spectral analysis of *Fermi*-LAT gamma-ray bursts with known redshift and their potential use as cosmological standard candles

Feraol F. Dirirsa[1,*], Soebur Razzaque[1] and Frédéric Piron[2]
on behalf of the *Fermi*-LAT Collaboration

[1]Department of Physics, University of Johannesburg, P. O. Box 524, Auckland Park 2006, South Africa

[2]Laboratoire Univers et Particules de Montpellier, Université de Montpellier, CNRS/IN2P3, place Eugène Bataillon, 34095 Montpellier cedex 5, France

E-mail: *fdirirsa@uj.ac.za

Abstract. Long duration Gamma-Ray Bursts (GRBs) may serve as new standard candles to constrain cosmological parameters by probing the Hubble diagram well beyond the range of redshift currently accessible using type-Ia supernovae. The standardization of GRBs is based on relations which correlate two or more parameters, found from gamma-ray spectral modelling, of which one is strongly dependent on the cosmological model. Amati relation, in particular, is between the source rest frame energy ($E_{i,p}$) at which the prompt gamma-ray spectral energy distribution peaks and the isotropic-equivalent bolometric energy (E_{iso}). We have selected a sample of 23 long GRBs (LGRBs) and 2 short GRBs (SGRBs) with known redshifts, which have been detected by the *Fermi* GBM and LAT instruments in eight years of operations, from July 2008 to December 2016. We have derived $E_{i,p}$ and E_{iso} for these LGRBs and SGRBs using the GBM and LAT data in joint spectral fits, often requiring multiple components, thus extending the computation of E_{iso} to the GeV range. Our results show that LGRBs detected by the *Fermi*-LAT with significant GeV emission are consistent with the Amati relation. These results further enhance the possibility to use the GRBs as cosmological standard candles.

1. Introduction

Gamma-ray bursts (GRBs) are energetic astronomical events that can be observed from redshift (z) up to ~ 9.4 [1]. High redshift GRBs may be used for gathering information of the cosmological evolution of the universe, which has been difficult to retrieve by other cosmological probes. According to observations, the GRBs can be classified as either long GRBs (LGRBs) lasting for more than 2 seconds or short GRBs (SGRBs) lasting for less than or equal to 2 seconds [2]. The limit between the diverse population of SGRBs and LGRBs are inferred through the observed durations T_{90} (i.e. the time to accumulate between 5% and 95% of the total counts in the burst). The LGRBs are perceived as a highly promising tool to probe the process of cosmological parameters, like the Type Ia Supernova (SNe Ia) [4]. The high-energy emission of LGRBs has been studied with the Energetic Gamma-Ray Experiment Telescope (EGRET) that covers the energy range from 30 MeV to 30 GeV [5]. Since 2008 the *Fermi*-Large Area Telescope (LAT) opened a new era for the study of high energy emission from GRBs [3] that detected more than

135 GRBs until July 2017. The two *Fermi* telescopes, the GRB Monitor (GBM) [6] and LAT [7], span an energy band from 8 keV to above 300 GeV. The GBM comprises of 12 Sodium Iodide (NaI) devices covering energies from 8 keV to 1 MeV and a pair of Bismuth Germanate (BGO) detectors (b0 and b1) covering energies from 200 keV to 40 MeV. Observations of the GRB prompt emission led to several phenomenological correlations among the emission properties. One of the most studied one is the Amati relation [8] that correlates the isotropic radiated energy (E_{iso}) in the 1-10^4 keV energy band and the photon energy of the νF_ν spectrum, both computed in the GRB rest frame. Many studies have been performed to test this correlation using various samples of LGRBs, collected from different gamma-ray telescopes [9, 10, 11, 12]. The results from those studies show that the $E_{i,p} - E_{iso}$ correlation may be used as a redshift estimator for GRBs [13] to constrain the cosmological parameters.

Since the spectra of GRBs detected by the *Fermi*-LAT/GBM extend up to a few tens of GeV in the cosmological rest-frame, the commonly adopted E_{iso} computation in the 1 keV - 10 MeV band is rather narrow, thus biasing the correlation. The samples of LGRBs used to compute the correlation were also collected from the telescopes with narrow energy bands with the peak of the spectrum outside the observed energy window [14]. Therefore, the joint *Fermi* GBM-LAT sample is valued for the correlation study by providing extended energy coverage to characterize a peak energy as well as validate the E_{iso} integrated over the energy range from 1 keV to 100 MeV. In this study, we assess a sample of 23 *Fermi* LGRBs and 2 SGRBs observed up to the LAT energy range until December 2016. For these data, the correlation between $E_{i,p}$ and E_{iso} in the cosmological rest frame have been studied.
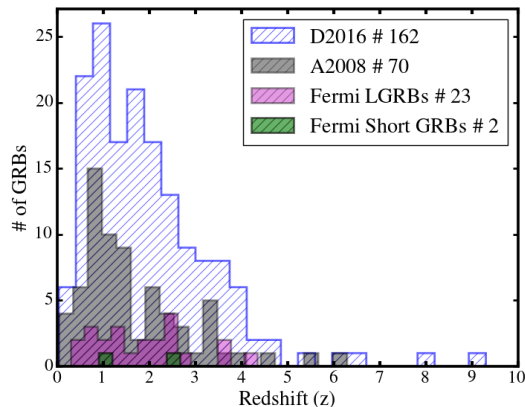

Figure 1. The redshift distributions of GRBs used by Amati et al. 2008 (A2008) [10], Demianski et al. 2016 (D2016) [15], *Fermi* LGRBs (magenta hatch) and *Fermi* SGRBs (green hatch). The list of *Fermi* LGRBs and SGRBs with redshift are given in Table 2.

2. Sample and data analysis

We conduct our analysis on the *Fermi* sample of 23 LGRBs and 2 short GRBs with identified redshift z. Their redshifts are derived from photometric or optical spectroscopy or calculated theoretically (i.e. estimate a redshift of ~1.55 for GRB 131014A [16]) covering the time period until December 2016. For GRB 110721A, the possibility that the object is an early-type galaxy at $z = 3.512$ has been considered (E. Berger GCN 12193, 2011). We use data from the GBM NaI detectors that have source angles less than 50 degrees, the data of BGO detector closer to the source and the LAT data. In order to subtract the GBM background spectrum for the spectral analysis, we have defined two background intervals before and after the prompt emission for each

energy channel. For each emission episode, we fit the spectrum with a second-order polynomial function to a user-defined background and interpolate this fit across the source interval. We have used the standard 128 energy bins of the CSPEC data-type, for NaI using the channels from ∼8 keV to ∼900 keV cutting out the over-flow high energy channels (corresponding to the Iodine K-edge from ∼30 ∼40 keV, see [6]). For BGO, we have used data from ∼220 keV to ∼40 MeV and ∼210 keV to ∼40 MeV for b1 and b0, respectively. For the LAT analysis, we have used the pass-8 data with Transient class events (`Transient20E`) by selecting them from within a 10-degrees radius of interest. The data is binned in 30 logarithmically spaced energy steps between 30 MeV and 300 GeV. Since, we consider energies below 100 MeV, the `gtlike` tool was used for the binned maximum-likelihood analysis of the data which offers the possibility to account for correcting the energy dispersion effect. We derive the observed spectrum and the detector response matrix using the *Fermi* Science Tools `gtbin` and `gtrspgen`. To produce a background spectrum file, the background estimation tool `gtbkg` was used.

For the spectral analysis, we have considered different functions because of the variety of spectral models that constrain the emission for the T_{90} duration as reported in Table 1. The fits are composed of three main components: (a) Band model (Band) [17], which smoothly connects two power laws joined by an exponential cutoff, (b) the low energy power law with an exponential high energy cutoff, so called Comptonized (Comp), and (c) the smoothly broken power-law (SBPL) [18]. We have also considered additional components in our spectral fits [19]: (I) the power law (PL) $dN/dE(E|A, \alpha_1) = A(E/100\ keV)^{\alpha_1}$, where α_1 is the photon index, and (II) the Black Body model (BB) $dN/dE(E|A, kT) = AE^2/(\exp(E/kT) - 1)$, where kT is the thermal temperature.

Table 1. The GRB names, triggers and the spectral fit parameters for 25 *Fermi* GRBs

GRB name	Triggers	Model	$T_{05} - T_{95}$	α or γ	β	E_p or E_0	kT	α_1	C-Stat/dof(*)
GRB 160625B	n7+n9+b1+LAT	Band+BB+PL	188.45-650.54	-0.40 ± 0.06	-2.70 ± 0.02	642.92 ± 15.48	27.94 ± 1.09	-2.16 ± 0.04	1462.9/354
GRB 160521B	n6+n7+n8+b1+LAT	Band	0.32-3.14	-0.48 ± 0.03	-2.62 ± 0.06	161.62 ± 4.16			547.15/468
GRB 160509A	n0+n1+n3+b0+LAT	Band+	7.68-379.4	-0.87 ± 0.08	-5.16 ± 0.49	8591.48 ± 68.27			
		Comp+PL		-0.79 ± 0.04		317.14 ± 16.60		-1.76 ± 0.10	1741.9/474
GRB 150514A	n3+n6+n7+b0+LAT	Band	0.00-10.8	-1.45 ± 0.08	-2.33 ± 0.05	76.28 ± 8.26			590.57/472
GRB 150403A	n3+n4+b0+LLE	Band+BB	3.33-25.60	-1.02 ± 0.02	-2.95 ± 0.10	793.63 ± 52.55	33.30 ± 1.58		524.75/358
GRB 150314A	n0+na+n1+n9+b1+LAT	Band	0.6-11.29	-0.63 ± 0.01	-3.02 ± 0.10	357.38 ± 4.78			1333.0/588
GRB 141028A	n6+n7+n9+b1+LAT	Band	6.66-38.16	-0.91 ± 0.02	-2.37 ± 0.02	396.45 ± 15.29			691.79/473
GRB 140619B	n1+n9+b1+LAT	SBPL	0.00-1.41	-0.46 ± 0.21	-2.28 ± 0.07	1428.7 ± 306.7			416.86/362
GRB 131231A	n0+n3+n7+b0+LAT	Band	13.31-44.31	-1.23 ± 0.01	-2.65 ± 0.03	225.17 ± 3.02			1665.0/476
GRB 131108A	n0+n3+n6+n7+b0+b1+LAT	SBPL	0.32 - 19.32	-0.99 ± 0.02	-2.23 ± 0.01	205.32 ± 6.91			950.58/716
GRB 131014A	n9+na+nb+b1+LAT	Band+BB	0.96-4.16	-0.40 ± 0.01	-2.85 ± 0.03	418.39 ± 6.99	33.53 ± 0.85		791.75/469
GRB 130518A	n3+n6+n7+b0+b1+LAT	Band	9.9-57.9	-0.89 ± 0.01	-2.71 ± 0.03	458.85 ± 9.22			1357.1/592
GRB 130427A	n6+n9+na+b1+LAT	Band+PL	11.23-142.34	-1.41 ± 0.01	-2.27 ± 0.01	219.61 ± 4.38		-1.22 ±0.21	2105.1/488
GRB 120624B	n1+n2+na+b0+b1+LAT	SBPL	-258.05-13.31	-1.04 ± 0.01	-2.78 ± 0.04	379.49 ± 8.15			2015.7/588
GRB 110731A	n0+n1+n6+n7+n9+b0+b1+LAT	Band+PL	0 - 7.3	-0.24 ± 0.10	-2.43 ± 0.08	260.70 ± 11.12		-1.95 ± 0.04	1277.9/826
GRB 110721A	n6+n7+n9+b1+LAT	Band	0.45 - 24.9	-1.12 ± 0.01	-2.60 ± 0.03	780.87 ± 43.32			666.74/473
GRB 100414A	n7+n9+n11+b1+LAT	Band	2.0 - 28.4	-0.50 ± 0.02	-2.91 ± 0.06	578.89 ± 11.69			750.82/469
GRB 091208B	n10+n9+b1+LAT	Band	0.26 - 15.26	-1.29 ± 0.07	-2.53 ± 0.12	98.22 ± 9.74			422.09/351
GRB 091003A	n0+n3+n6+b0+b1+LAT	Band	1.09 - 22.19	-1.08 ± 0.01	-2.79 ± 0.05	452.21 ± 17.44			674.54/600
GRB 090926A	n6+n7+n8+b1+LAT	SBPL	2.05-22.05	-0.90 ± 0.01	-2.27 ± 0.01	171.50 ± 2.36			945.02/478
GRB 090902B	n0+n2+n9+b0+b1+LAT	Band+PL	0-22	-0.53 ± 0.01	-4.14 ± 0.28	760.66 ± 7.69		-1.92 ± 0.01	1320.6/601
GRB 090510	n3+n6+n7+n9+b0+b1+LAT	SPBL	0.002: 1.744	-0.86 ± 0.03	-2.26 ± 0.03	1873.00 ± 212.70			788.82/720
GRB 090328	n7+n8+b1+LAT	Band	4.67-61.67	-1.04 ± 0.02	-2.37 ± 0.04	703.75 ± 47.16			769.08/360
GRB 090323	n6+n7+n9+n11+b1+LAT	SBPL	-1.0 - 173	-1.29 ± 0.01	-2.50 ± 0.02	399.44 ± 17.17			1558.6/597
GRB 080916C	n3+n4+b0+LAT	SBPL	0 - 66	-1.11 ± 0.01	-2.20 ± 0.01	270.46 ± 12.20			579.20/364

Notes. α and β are the lower and higher photon indices for Band and SBPL functions, respectively. E_0 is the SBPL e-folding energy in keV. γ is the photon index of Comp. E_p is the Band or Comp peak energy in keV. C-Stat/dof(*) is the ratio of the value of the C-stat resulting from the fit and the associated degrees of freedom (dof)−This results cannot be used to estimate goodness of fit nevertheless compare to C-stat for models.

3. Testing the $E_{i,p} - E_{iso}$ correlation for the bright *Fermi* GRBs

To measure the fitting parameters generated by the `rmfit` package and uncertainty on those parameters, we use Monte Carlo simulations by assuming the parameters follow a multivariate Gaussian function. Using the covariance matrix obtained from the spectral fit, 10,000 sets of random values were generated for the parameters and the most probable value of the final

distribution with 68.27% confidence interval was selected. These results are reported in Tables 1 and 2. The E_{iso} and $E_{i,p}$ are also chosen as the most probable values of the final distributions, and errors derived from the 1σ confidence interval around these values are reported in Table 2.

Table 2. Analysis of $E_{i,p}$ and E_{iso} in the GRB rest-frame

GRB name	z	$E_{i,p}$ (keV)	E_{iso}^{+} (erg)	E_{iso}^{++} (erg)
GRB 160625B	1.406^a	1546.86 ± 37.25	$(4.35 \pm 0.06) \times 10^{54}$	$(4.94 \pm 0.07) \times 10^{54}$
GRB 160521B	$z > 2.5^b$	565.67 ± 14.55	$(1.71 \pm 0.03) \times 10^{53}$	$(1.85 \pm 0.06) \times 10^{53}$
GRB 160509A	1.17^c	19334.10 ± 652.25	$(1.83 \pm 0.05) \times 10^{54}$	$(3.65 \pm 0.14) \times 10^{54}$
GRB 150514A	0.807^d	137.84 ± 14.93	$(1.26 \pm 0.05) \times 10^{52}$	$(1.37 \pm 0.07) \times 10^{52}$
GRB 150403A	2.06^e	2428.51 ± 160.80	$(8.52 \pm 0.18) \times 10^{53}$	$(9.53 \pm 0.27) \times 10^{53}$
GRB 150314A	1.758^f	985.66 ± 13.20	$(7.27 \pm 0.10) \times 10^{53}$	$(7.60 \pm 0.17) \times 10^{53}$
GRB 141028A	2.33^g	1320.18 ± 50.90	$(6.40 \pm 0.07) \times 10^{53}$	$(7.98 \pm 0.12) \times 10^{53}$
GRB 140619B	2.67 ± 0.37^h	5192.46 ± 1210.86	$(4.38 \pm 1.12) \times 10^{52}$	$(8.03 \pm 2.37) \times 10^{52}$
GRB 131231A	0.6439^i	370.15 ± 4.97	$(1.92 \pm 0.01) \times 10^{53}$	$(2.01 \pm 0.02) \times 10^{53}$
GRB 131108A	2.40^j	1163.20 ± 28.54	$(1.14 \pm 0.04) \times 10^{54}$	$(1.53 \pm 0.05) \times 10^{54}$
GRB 131014A	$\sim 1.55^k$	1066.90 ± 17.83	$(1.14 \pm 0.01) \times 10^{54}$	$(1.22 \pm 0.01) \times 10^{54}$
GRB 130518A	2.49^l	1601.40 ± 32.19	$(1.67 \pm 0.02) \times 10^{54}$	$(1.89 \pm 0.02) \times 10^{54}$
GRB 130427A	0.3399^m	294.25 ± 5.86	$(9.29 \pm 0.06) \times 10^{52}$	$(1.06 \pm 0.01) \times 10^{53}$
GRB 120624B	0.57 ± 0.07^n	595.02 ± 20.37	$(1.85 \pm 2.74) \times 10^{53}$	$(1.96 \pm 2.94) \times 10^{53}$
GRB 110731A	2.83^o	998.47 ± 42.59	$(4.86 \pm 0.11) \times 10^{53}$	$(5.98 \pm 0.23) \times 10^{53}$
GRB 110721A	3.512^p	3523.30 ± 195.47	$(1.39 \pm 0.03) \times 10^{54}$	$(1.79 \pm 0.04) \times 10^{54}$
GRB 100414A	1.368^q	1370.82 ± 27.68	$(5.87 \pm 0.08) \times 10^{53}$	$(6.35 \pm 0.12) \times 10^{53}$
GRB 091208B	1.063^r	202.63 ± 20.10	$(2.26 \pm 0.12) \times 10^{52}$	$(2.37 \pm 0.17) \times 10^{52}$
GRB 091003A	0.8969^s	857.81 ± 33.08	$(9.58 \pm 0.16) \times 10^{52}$	$(1.02 \pm 0.02) \times 10^{53}$
GRB 090926A	2.1062^t	861.41 ± 8.52	$(1.95 \pm 0.01) \times 10^{54}$	$(2.50 \pm 0.02) \times 10^{54}$
GRB 090902B	1.822^u	2146.57 ± 21.71	$(3.29 \pm 0.02) \times 10^{54}$	$(3.49 \pm 0.03) \times 10^{54}$
GRB 090510	0.903^v	5927.47 ± 459.00	$(3.69 \pm 1.45) \times 10^{51}$	$(6.75 \pm 3.23) \times 10^{51}$
GRB 090328	0.736^w	1221.71 ± 81.87	$(1.16 \pm 0.03) \times 10^{53}$	$(1.42 \pm 0.05) \times 10^{53}$
GRB 090323	3.57^x	2060.23 ± 138.07	$(4.30 \pm 0.10) \times 10^{54}$	$(5.35 \pm 0.17) \times 10^{54}$
GRB 080916C	4.35 ± 0.15^y	2434.39 ± 108.43	$(3.57 \pm 0.14) \times 10^{54}$	$(5.33 \pm 0.19) \times 10^{54}$

Notes. E_{iso}^{+} and E_{iso}^{++} are computed in the $1 - 10^4$ keV and $1 - 10^5$ keV energy range of cosmological rest frame by assuming a standard ΛCDM cosmology with $H_0 = 69.6$ km s^{-1} Mpc^{-1}, $\Omega_m = 0.286$ and $\Omega_\Lambda = 0.714$, respectively.
References for the redshift: (a) Xu et al. GCN 19600 (2016); D'Elia et al. GCN 19601 (2016), (b) Ruffini et al. GCN 19456 (2016), (c) Tanvir et al. GCN 19419 (2016), (d) de Ugarte Postigo et al. GCN 17822 (2015), (e) Pugliese et al. GCN 17672 (2015); Golenetskii et al. GCN 17677 (2015), (f) de Ugarte Postigo et al. GCN 17583 (2015); Golenetskii et al. GCN 17587 (2015), (g) Xu et al. GCN 16983 (2014), (h) Ruffini et al. ApJ 808 190 (2015), (i) Xu et al. GCN 15645 (2013); Cucchiaras GCN 15652 (2013), (j) de Ugarte Postigo et al. GCN 15470 (2013); Golenetskii et al. GCN 15480 (2013), (k) Guiriec et al. (2015), (l) Snchez-Ramrez et al. GCN 14685 (2013); Cucchiara et al. GCN 14687 (2013), (m) Xu et al. 776 98 (2013), (n) de Ugarte Postigo et al. GCN 13395 (2012), (o) Tanvir et al. GCN 12225 (2011), (p) Berger GCN 12193 (2011); Grupe et al. GCN 12212 (2011), (q) Cucchiara and Fox GCN 10606 (2010), (r) Wiersema et al. GCN 10263 (2009), (s) Cucchiara et al. GCN 10031 (2009), (t) Malesani et al. GCN 9942 (2009); Cenko et al. GCN 10049 (2009), (u) Cucchiara et al. GCN 9873 (2009), (v) Rau et al. GCN 9353 (2009); Ackermann et al. (2010), (w) Cenko et al. GCN 9053 (2009), (x) Chornock et al. GCN 9028 (2009), and (y) Greiner et al. $A\&A$ 498 89 (2009).

The Amati relation between E_{iso} and $E_{i,p}$ can be parametrized as follows:

$$\log \frac{E_{i,p}}{\text{erg}} = k + m \log \frac{E_{iso}}{\text{keV}}, \tag{1}$$

where k and m are the intercept and slope of this linear equation. For notation, we define $x = \log \frac{E_{iso}}{\text{erg}}$ and $y = \log \frac{E_{i,p}}{\text{keV}}$, and fit the correlated data $\{x_i, y_i\}$ with uncertainties $\{\sigma_{xi}, \sigma_{yj}\}$, to the linear relation $y = k + mx$. Following the description of Wang et al. (2015) [20], the parameter y should not only depend on x, but also depend on an extrinsic variance (σ_{ext}) to quantify the hidden cosmological parameters in E_{iso} through the luminosity distance (d_L). The optimal parameters (k, m and σ_{ext}) can be obtained by minimizing the chi-square function $\chi^2 = \sum_{i=0}^{N-1} (y_i - k - mx_i)^2/(\sigma_{yi}^2 + m^2\sigma_{xi}^2 + \sigma_{ext}^2)$, where N is the number of GRBs, such that the reduced $\chi^2 = 1$ [20]. This method gives a value for the parameter σ_{ext} to quantify the extrinsic error. The correlations coefficient for both energy range 1 - 10^4 keV and 1 - 10^5 keV corresponding to the 22 *Fermi* LGRBs are $\rho_{sp} = 0.79$ and $\rho_{sp} = 0.80$, respectively, which are very significant (see Table 3, column 4).
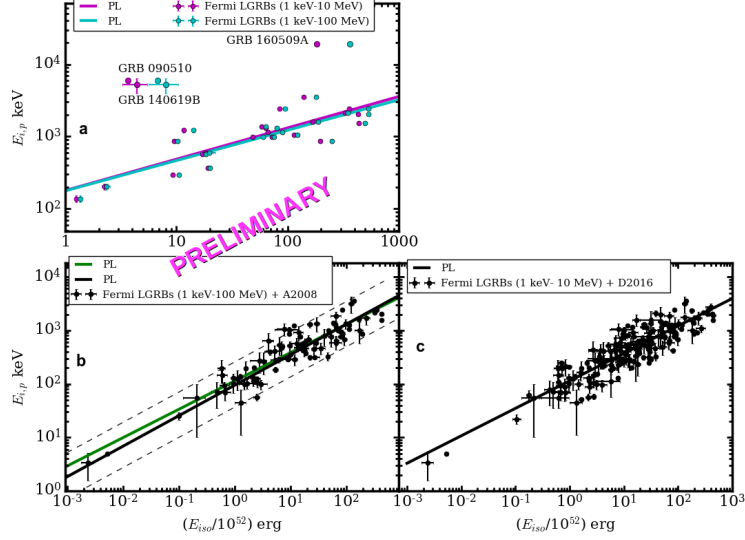
Figure 2. The Amati relation in the $E_{i,p}$ - E_{iso} plane. All the fitting lines are plotted over the data points when the reduced χ^2 is unity. In panel a) the magenta and cyan lines represent the fits to the *Fermi* LGRBs data with E_{iso} computed for (1 keV -10 MeV) and (1 keV - 100 MeV), respectively. In panel b) the green line depict the fit to the joint A2008 and *Fermi* LGRBs data, the black line show the A2008 fit and black dashed lines are the 2σ scatter limits of $E_{i,p}$ - E_{iso} correlation [10]. In panel c) the black line shows the fit to the joint D2016 and *Fermi* LGRBs (1 keV - 10 MeV) data. The fit parameters are reported in Table 3.

Table 3. The results of the $E_{i,p}$ - E_{iso} correlation fitting data when the reduced χ^2 is unity.

Figure	Reference	N	ρ_{sp}	m	k	σ_{ext}
a	*Fermi* LGRBs (1 keV - 10 MeV)	22	0.79	0.434 ± 0.071	178.858 ± 54.18	0.197 ± 0.022
	Fermi LGRBs (1 keV - 100 MeV)	22	0.80	0.420 ± 0.066	176.932 ± 53.105	0.194 ± 0.021
b	*Fermi* LGRBs + A2008	92	0.88	0.529 ± 0.027	112.790 ± 10.305	0.194 ± 0.027
c	*Fermi* LGRBs + D2016	184	0.87	0.513 ± 0.023	113.800 ± 8.125	0.205 ± 0.016

We have also estimated the free parameters (k, m and σ_{ext}) by using the combined *Fermi* LGRBs, A2008 and D2016 data sets. As an example, by using the reduced χ^2 for 22 *Fermi* LGRB data (E_{iso} computed in 1 keV - 10 MeV), the estimated value of k, m and σ_{ext} are $\sim$181.628, $\sim$0.430 and $\sim$0.26, respectively. When the reduced χ^2 is $\sim$ 1, the parameters k and σ_{ext} are reduced to 178.858 and 0.197, respectively. In Fig. 2a), we find SGRBs 140619B and 090510 as clear outliers of the correlations in the $E_{i,p} - E_{iso}$ plane. Long GRB 160509A is also considered as outlier due to the effect of joint spectral fitting by the Band and Comp functions. The peak energy obtained from this model [21] is higher in the $E_{i,p}$ - E_{iso} plane, but the effect on E_{iso} is insignificant. If we fit the data in Fig. 2b with a simple power law, we find an index $\sim$0.53 and a normalization $\sim$112, consistent with the results of previous analysis (e.g. Amati 2002). The best power law fit of the joint *Fermi* LGRBs (1 keV - 10 MeV) and D2016 data shown in Fig. 2c gives the index $\sim$0.51 and normalization $\sim$ 114 with the very significant Spearman's correlation coefficient $\rho_{sp} = 0.87$.

4. Conclusion

We have reported the correlation of $E_{i,p}$ and E_{iso} in the source rest frame for the GRBs with very high energy emission detected by the *Fermi*/LAT-GBM with known redshift. The spectral analysis has been performed using uniform time duration T_{90} and homogenous energy range selection. Using the parameters found from gamma-ray spectral modelling, $E_{i,p}$ and E_{iso} are computed which are strongly dependent on the cosmological model. The linear case with errors on both $E_{i,p}$ and E_{iso} axis, and extrinsic variance of the data has been shown, giving the χ^2 formula. The best-fit value of the parameter m is in the range 0.425-0.529, which can be compared to $m = 0.434$-0.513 obtained in all samples when the reduced χ^2 approaches to unity. Our results show that the *Fermi* LGRB emission, detected by LAT up to 10 MeV and 100 MeV, further provide a significant contribution to the study on the reliability of the Amati relation. In addition, we also found that LGRBs in the $E_{i,p} - E_{iso}$ plane follow similar correlation as measured using other instruments and short GRBs do not follow this correlation. Finally, the extremely energetic long GRB 080916C and GRB 090323 with significant GeV emission detected by the *Fermi*-LAT further confirm and extend the Amati relation with very high isotropic radiated energy $(5.33 \pm 0.19) \times 10^{54}$ erg and $(5.35 \pm 0.17) \times 10^{54}$ erg in the energy range 1 - 10^5 keV. We deduce that the *Fermi*-LAT/GBM GRBs with high energy emission are consistent with the Amati relation and could be used as effective cosmological standard candles.

References

[1] Cucchiara A *et al.* 2011 *The Astrophysical Journal* **736** 7
[2] Bissaldi E *et al.* 2011 *The Astrophysical Journal* **733** 97
[3] Gehrels N and Razzaque S 2013 *Frontiers of Physics* **8** 661–678
[4] Riess A G *et al.* 1998 *The Astronomical Journal* **116** 1009
[5] Fichtel C *et al.* 1994 *The Astrophysical Journal Supplement Series* **94** 551–581
[6] Meegan C *et al.* 2009 *The Astrophysical Journal* **702** 791
[7] Atwood W *et al.* 2009 *The Astrophysical Journal* **697** 1071
[8] Amati L *et al.* 2002 *Astronomy & Astrophysics* **390** 81–89
[9] Amati L 2006 *Monthly Notices of the Royal Astronomical Society* **372** 233–245
[10] Amati L *et al.* 2008 *Monthly Notices of the Royal Astronomical Society* **391** 577–584
[11] Ghirlanda G *et al.* 2005 *Monthly Notices of the Royal Astronomical Society: Letters* **361** L10–L14
[12] Heussaff V, Atteia J L and Zolnierowski Y 2013 *Astronomy & Astrophysics* **557** A100
[13] Atteia J L 2003 *Astronomy & Astrophysics* **407** L1–L4
[14] Sakamoto T *et al.* 2009 *The Astrophysical Journal* **693** 922
[15] Demianski M, Piedipalumbo E, Sawant D and Amati L 2017 *Astronomy & Astrophysics* **598** A112
[16] Guiriec S *et al.* 2015 *The Astrophysical Journal* **814** 10
[17] Band D *et al.* 1993 *The Astrophysical Journal* **413** 281–292
[18] Ryde F 1999 *Astrophysical Letters and Communications* **39** 281 (*Preprint* `astro-ph/9811462`)
[19] Guiriec S *et al.* 2015 *The Astrophysical Journal* **807** 148
[20] Wang J, Wang F, Cheng K and Dai Z 2016 *Astronomy & Astrophysics* **585** A68
[21] Guiriec S *et al.* 2011 *The Astrophysical Journal Letters* **727** L33